Noise reduction and aerodynamics of airfoils with porous trailing edges

Thomas F. Geyer[1]
Technical Acoustics Group, Brandenburg University of Technology Cottbus - Senftenberg
03046 Cottbus, Germany

Ennes Sarradj[2]
Institute of Fluid Mechanics and Engineering Acoustics, Technische Universität Berlin
10587 Berlin, Germany

ABSTRACT

The application of open-porous materials is one possible method to reduce the aerodynamic noise of an airfoil. Depending on the exact location and extent of the porous region, it enables the reduction of trailing edge noise or of noise from the leading edge when subject to inflow turbulence. However, the porous consistency may have a negative effect on the aerodynamic performance of the airfoil, since very often the lift is decreased while the drag increases. In a recent investigation, the generation of trailing edge noise of a set of airfoil models made from different porous materials was examined experimentally. The materials were characterized by their air flow resistivity. Besides the material, the chordwise extent of the porous material was varied. Acoustic measurements were performed in an open jet wind tunnel using microphone array technology, while the aerodynamic performance was measured simultaneously using a six-component balance. In general, both the air flow resistivity and the extent of the porous material have an influence on the trailing edge noise. However, if a suitable material is chosen, the results show that a noticeable reduction of trailing edge noise is possible even with only a small extent of the porous material.

Keywords: Airfoil trailing edge noise, Porous material, Wind tunnel

1. INTRODUCTION

Airfoil trailing edge noise is a dominant source of noise in several applications, including wind turbine noise, fan noise and airframe noise. There are different methods to reduce this noise source by modifying the blade, which includes the use of flow permeable materials. Several studies on this passive modification exist, including experimental studies on brush-like or slitted trailing edge extensions [1–3], on fully porous airfoils [4, 5] and on airfoils with trailing edges modified by metal mesh sheets [7] or porous foams [8, 9]. There are also approaches to combine the successful concept of serrated trailing edges with a porous modification [10]. In addition, there are a variety of analytical [11] and numerical studies [12–15] on porous trailing edges for noise reduction available. The present paper is a continuation of an investigation of so-called *partially porous airfoils* described in [16], where the front part of the airfoil is non-porous and only the trailing edge is permeable to the flow. The aim of this design is to combine the aerodynamic advantages of a conventional, non-porous airfoil with the acoustic advantages of a fully porous airfoil.

2. MATERIALS AND METHODS

All experiments were performed in the small aeroacoustic wind tunnel at the Brandenburg University of Technology in Cottbus using microphone array technique and a wind tunnel balance.

[1]email: thomas.geyer@b-tu.de
[2]email: ennes.sarradj@tu-berlin.de

Table 1: Materials used for the manufacturing of the airfoils (given is the air flow resistivity r, measured according to ISO 9053 [17])

Name	Material	r in Pa s/m^2
Reference	non-porous	∞
Porex	polyethylene granulate	316,500
Siperm R200	metal foam	150,000
Damtec estra	rubber granulate	86,100
Damtec USM	rubber granulate	12,900
Recemat	metal foam	8,200
M-Pore Al 45 ppi	metal foam	1,000

2.1 Airfoils

The airfoils of the present study had an SD7003 shape with a chord length c_l of 235 mm and a span width b of 400 mm. The porous materials are characterized by their air flow resistivity

$$r = \frac{\Delta p \cdot A}{q \cdot h}, \tag{1}$$

which was determined according to ISO 9053 [17] for cylindrical samples of the material with a diameter of 100 mm and thickness h. A is the resulting cross sectional area of the sample, Δp is the pressure difference across the sample and q is the volume rate of the flow through the material. Although there exist various other parameters to describe the properties of homogeneous porous materials, such as the porosity σ and the tortuosity τ, it is believed that the air flow resistivity is one of the most important regarding the potential noise reduction ability.

Since it was found as a result of a previous study on porous trailing edges [16] that materials with medium to high air flow resistivity are especially promising regarding a potential noise reduction, new porous materials were acquired in addition to the ones used in [16]. This includes two airfoils made from a rubber granulate with medium air flow resistivities (Damtec estra, r = 86,100 Pa s/m^2 and Damtec USM, r = 12,900 Pa s/m^2) as well as an airfoil made of a metal foam with a high air flow resistivity (Siperm R200, r = 150,000 Pa s/m^2). An overview of all airfoils of the present study is given in Table 1.

The airfoils were manufactured from spanwise slices of porous material, which were cut from plates of the porous materials using water jet cutting, since other technologies like laser cutting or milling would most likely close the open pores on the surface. However, it was found that for some of the porous materials even the water cutting may have affected the pores on the surface. This would lead to a different permeability through the airfoil compared to that of a homogeneous porous material. For example, the surface of the porous airfoil made of the new material Siperm R200, a stainless steel foam with a nominal porosity of 49 % to 54 % and a pore size of 65 μm, was definitely changed due to the water jet cutting, which is shown in Figure 1. It seems that the porosity on the surface is reduced, which would lead to a notably reduced permeability.

Thus, in order to examine the possible influence of the water jet cutting and to obtain a characteristic value for the permeability of the airfoil anyway, the air flow resistance [17]

$$R = \frac{\Delta p}{q} = \frac{p_+ - p_0}{q}, \tag{2}$$

was measured for all of the airfoils from Table 1. In Eq. (2), p_+ is the positive air pressure and p_0 is the ambient air pressure. The measurements were performed in situ using a special measuring head that was pressed against the upper surface of the airfoils (see schematic in Figure 2(a)). In order to prevent air leakage between the measurement head and the airfoil surface, a soft polyurethane foam, covered by an impermeable thin plastic film, was used as sealing. In total, the air flow resistance R was measured at three chordwise stations of x/c_l = 20 %, 50 % and 70 %. At each station, ten measurements were done along the span and the data were averaged. The results are shown as a function of r in Figure 2(b). It is visible that the airfoil made of Damtec estra (r = 86,100 Pa s/m^2) has an unexpectedly low air flow resistivity, which might be due to small slits between adjacent slices of the material. As expected, it seems that the air flow resistance of the

(a) Surface of the homogeneous *sample*

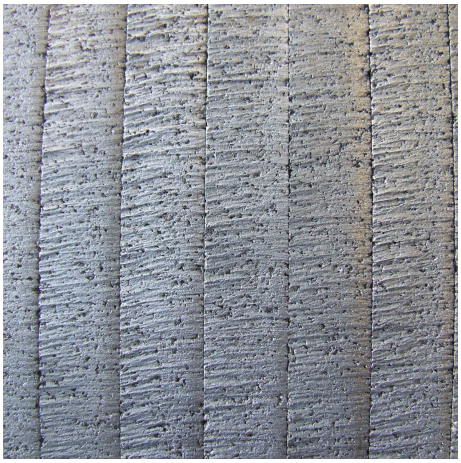

(b) Surface of the porous airfoil

Figure 1: Modification of the surface of the airfoil made of Siperm R200 due to the water jet cutting

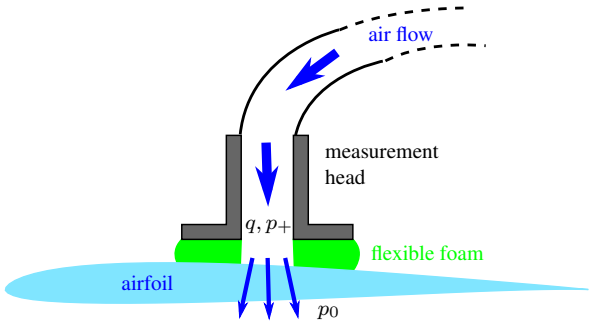

(a) Schematic of the setup used for the air flow resistance measurements (not to scale)

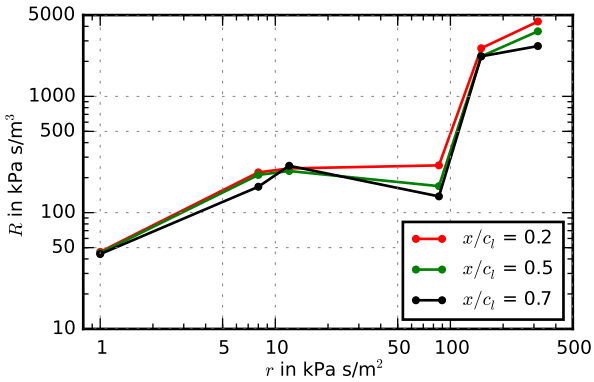

(b) Relation between air flow resistance R at different chordwise positions and air flow resistivity r

Figure 2: Air flow resistance R of the porous airfoils

airfoil made of Siperm R200 might be higher than expected based on the air flow resistivity r of the material. Still, in the remainder of this paper the air flow resistivity r will be used to characterize the porous airfoils.

It is known that flow permeable airfoils can lead to a noticeable noise reduction compared to a non-porous reference airfoil, while at the same time the aerodynamic performance will be reduced [4, 5]. One approach to improve the aerodynamics, that was also used in [16], is to cover a large part of the porous airfoil surface with a thin, impermeable foil and leave only the trailing edge porous (see Figure 3). This method was also employed in the current study, using the foils *Oracal Banner Cal 451*, *Oracal Exhibition Cal 631* and *Oracal Intermediate Cal 651* to cover the surface of the porous airfoils. Thus, different chordwise extents s/c_l of 5 %, 10 %, 20 %, 30 %, 50 % and 100 % (fully porous) were realized. In addition, a non-porous airfoil was used as a reference. The partially porous airfoils and the reference airfoil were tripped at 10 % of the chord using *Anti-slip tape* with a height of approximately 0.8 mm and a width of 2 mm. No tripping tape was applied to the fully porous airfoils since their relatively coarse surface ensured the existence of a turbulent boundary layer.

2.2 Wind Tunnel

The aeroacoustic wind tunnel at BTU [18] is an open jet wind tunnel, driven by a radial fan with a shaft power of 18.5 kW. The circular nozzle used in this study has a diameter of 0.2 m and enables a maximum flow speed in the order of 90 m/s. The airfoils were mounted with their leading edge 0.05 m downstream from the nozzle exit area. During acoustic measurements, the test section in front of the nozzle is surrounded on

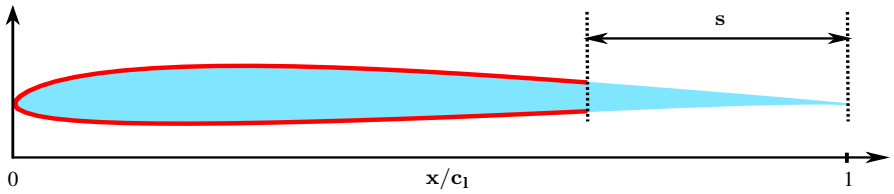

Figure 3: Schematic of a partially porous airfoil (light blue: porous airfoil, red: flexible, impermeable foil used to cover the pores at the front part of the airfoil, s: chordwise extent of the porous material)

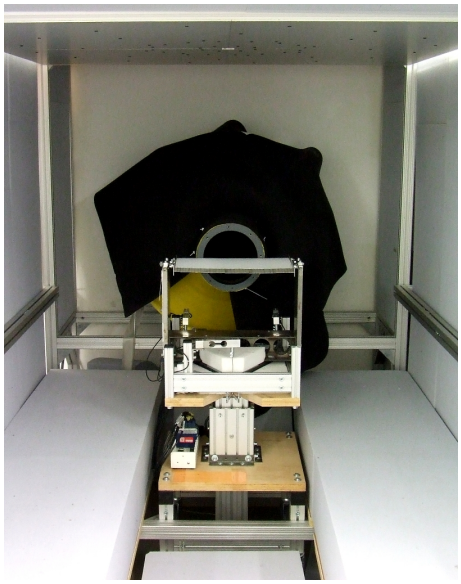

(a) Photograph (taken from downstream)

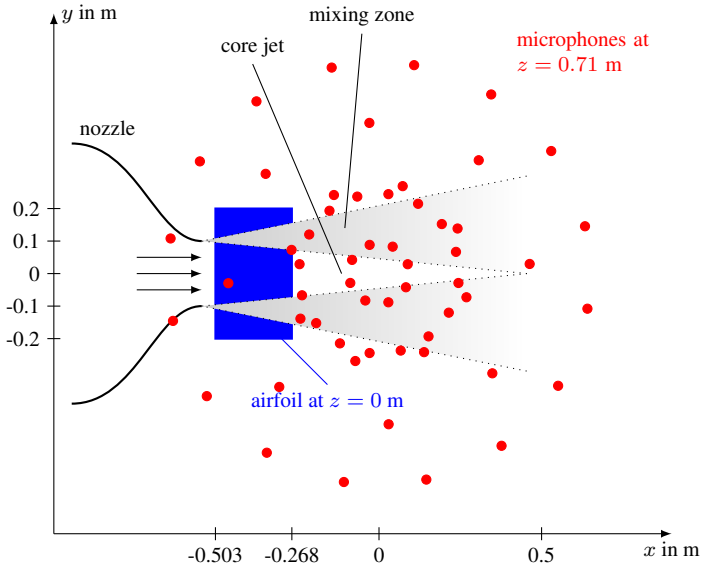

(b) Schematic of the measurement setup (top view)

Figure 4: Experimental setup in the aeroacoustic wind tunnel

three sides by absorbing walls, which are covered by 0.24 m thick absorber plates that lead to quasi anechoic measurement conditions at frequencies above 125 Hz. Figure 4(a) shows a photograph of the measurement setup.

2.3 Microphone Array and Data Processing

All acoustic measurements were performed using a planar microphone array, consisting of 56 1/4th inch microphones flush-mounted in a 1.5 m × 1.5 m large aluminum plate. The array was positioned 0.71 m above the airfoil and out of the flow (see Figure 4(b)). 40 s of data were recorded for each measurement with a sampling frequency of 51.2 kHz using a 24 Bit National Instruments multichannel measurement system and stored on a RAID server.

In post-processing, the time data were first transferred to the frequency domain using a Fast Fourier Transformation. This was done on 50 % overlapping Hanning-windowed blocks of 4,096 samples each. The resulting microphone auto spectra and cross spectra, that have a frequency resolution of 12.5 Hz, were then averaged to obtain the final cross spectral matrix. In order to separate the different noise sources, the CLEAN-SC deconvolution beamforming algorithm [19] was applied to the cross spectral matrizes. This was done on a fully three-dimensional focus grid. Thereby, the refraction of sound at the shear layer of the open jet was taken into account [20].

Finally, the noise contributions within a volume that contains only the part of the trailing edge interacting with the turbulent boundary layer, were integrated and converted to sound pressure level spectra. The noise from other, unwanted noise sources such as the interaction of the open jet shear layer with the leading edge and trailing edge of the airfoils, was excluded from the integration. Figure 5 shows a sample sound map that includes the chosen integration volume.

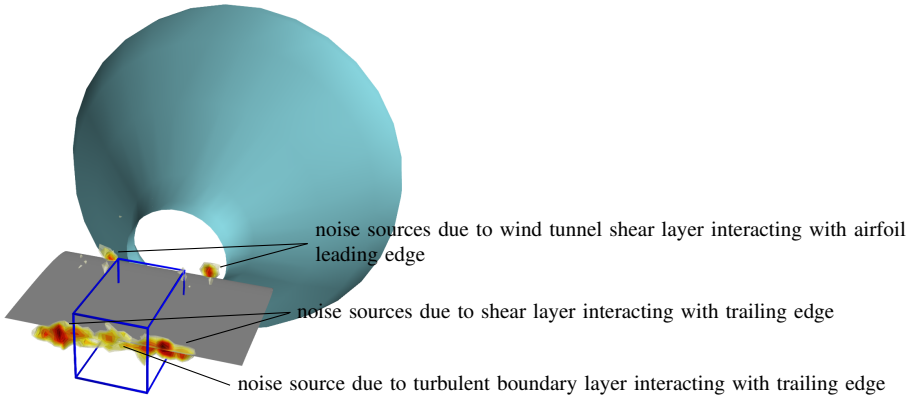

Figure 5: Sample sound map obtained for the reference airfoil, including several noise sources and the chosen integration volume (blue)

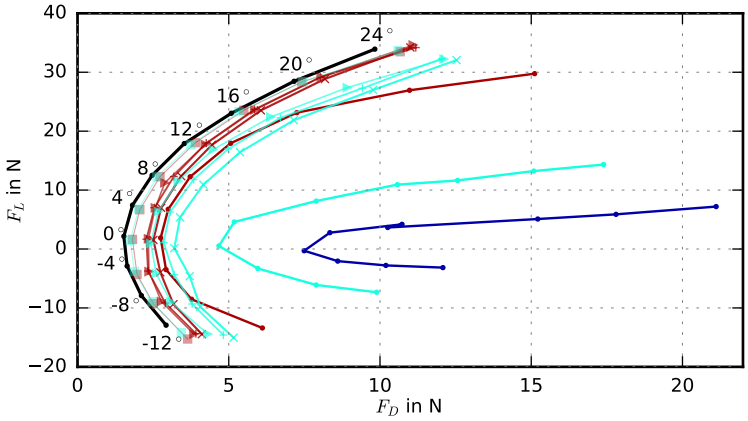

Figure 6: Overview of the aerodynamic performance of the partially porous airfoils as a function of angle of attack for a constant flow speed of 58 m/s (M = 0.168, Recemat, r = 8,200 Pa s/m^2, s/c_l = ■ 0.05, ▸ 0.2, + 0.3, × 0.5, ● 1; Porex, r = 316,500 Pa s/m^2, s/c_l = ■ 0.05, ▸ 0.2, + 0.3, × 0.5, ● 1; M-Pore Al, r = 1,000 Pa s/m^2, s/c_l = ● 1, ● non-porous reference airfoil, $r = \infty$)

2.4 Aerodynamic Measurements

In order to be able to take the aerodynamic performance of the partially porous airfoils into account, the lift and drag forces of the airfoils were measured simultaneously to the acoustic measurements. This was done using a six component balance (see Figure 4(a)) and in-house software.

3. RESULTS

The majority of the measurements was performed at a geometrical angle of attack of 4°, while aerodynamic measurements were also performed at additional angles. Due to an upgrade of the wind tunnel fan that took place after the experiments described in [16], the flow speed was now varied from approximately 18 m/s up to a maximum of 87 m/s, corresponding to Mach numbers M from 0.05 to 0.25 (subsonic flow).

3.1 Aerodynamic Results

In order to obtain a first understanding of the aerodynamic effect of the porous trailing edges, Figure 6 shows Lilienthal type polar diagrams for selected airfoils at geometrical angles of attack between -12° and 24°. As expected, it is visible that at any angle the reference airfoil generates the highest lift force F_L and the lowest drag force F_D. The basic trend that can be observed for the partially porous airfoils is that the lift force increases with increasing air flow resistivity r and decreasing extent s of the porous materials. For the drag force F_D, the opposite trend is found, it increases with decreasing r and increasing s.

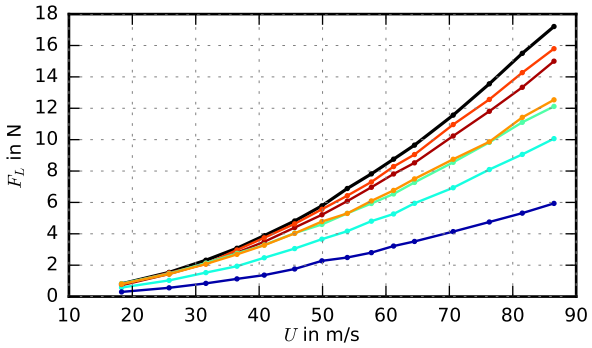

(a) Lift force as a function of flow speed

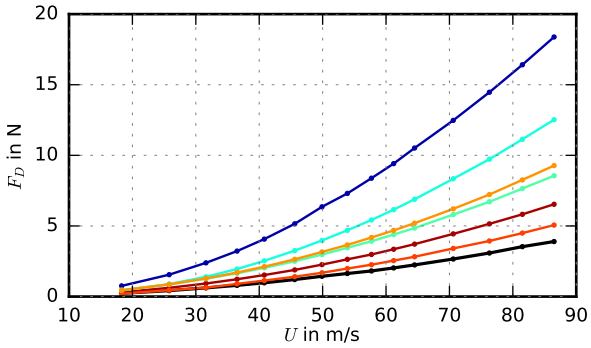

(b) Drag force as a function of flow speed

Figure 7: Influence of the material of the fully porous airfoils on the aerodynamic performance (● M-Pore Al, r = 1,000 Pa s/m^2, ● Recemat, r = 8,200 Pa s/m^2, ● Damtec USM, r = 12,900 Pa s/m^2, ● Damtec estra, r = 86,100 Pa s/m^2, ● Siperm R200, r = 150,000 Pa s/m^2, ● Porex, r = 316,000 Pa s/m^2, ● non-porous reference airfoil)

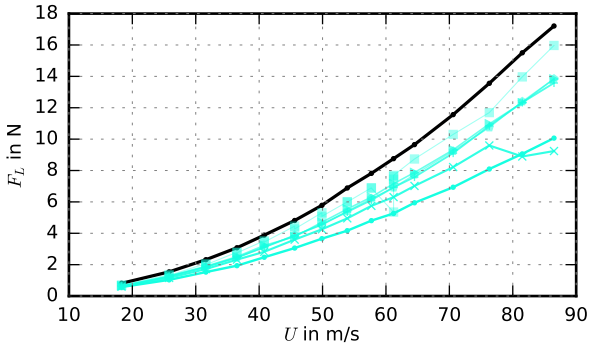

(a) Lift force as a function of flow speed

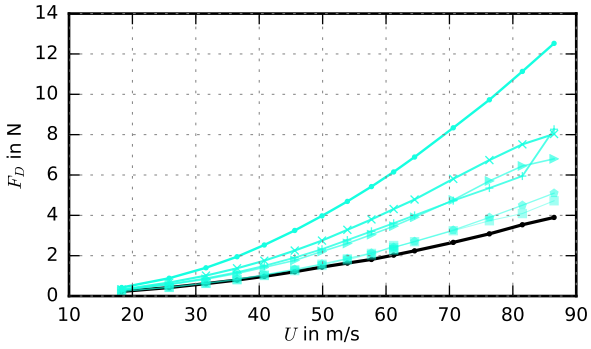

(b) Drag force as a function of flow speed

Figure 8: Influence of the streamwise extent s of the porous trailing edge on the aerodynamic performance (Recemat, r = 8,200 Pa s/m^2, s/c_l = ■ 0.05, ⬟ 0.1, ▶ 0.2, + 0.3, × 0.5, ● 1, ● non-porous reference airfoil)

The sole effect of the porous materials on the aerodynamic forces can be seen from Figure 7 for the fully porous airfoils (s/c_l = 1). Basically, the same conclusions can be drawn regarding the influence of r as from the previous Figure 6: When the air flow resistivity increases, the lift force F_L increases while the drag force F_D decreases. However, a close observation reveals an interesting detail regarding the airfoil made of Siperm R200. While technically it is the porous material with the second highest air flow resistivity of r = 150,000 Pa s/m^2 (second to Porex with r = 315,500 Pa s/m^2), it achieves the highest lift and the lowest drag of the porous airfoils. This can be assumed to be due to the change of the surface as a result of the water cutting, as described in Section 2.1. It seems that the water cutting, although not resulting in a much higher air flow resistance R (see Figure 2(b)), does improve the aerodynamic properties, maybe by making the surface smoother. In addition, as expected Figure 7 shows that the airfoil made of Damtec estra, which has a nominal air flow resistivity of 86,100 Pa s/m^2, generates less lift and more drag than the other porous airfoil made of a rubber granulate, Damtec USM with r = 12,900 Pa s/m^2. This is due to the differences in the air flow resistance R, as shown in Figure 2(b).

The sole effect of the extent s of the porous material on the aerodynamic forces is then shown in Figure 8 for the airfoil made of Recemat (r = 8,200 Pa s/m^2). As would be expected, the lift force increases with decreasing extent of the porous material, while the drag force decreases with decreasing s.

3.2 Acoustic Results

Sample sound maps are shown for selected airfoils at a single flow speed of 81.5 m/s in Figure 9. When examining these sound maps it has to be kept in mind that the noise source of interest is only the one positioned at

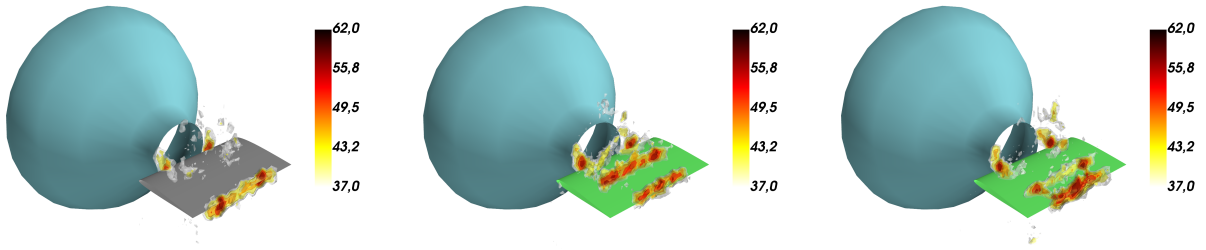

(a) Reference

(b) Recemat (r = 8,200 Pa s/m^2), s/c_l = 0.5

(c) Recemat (r = 8,200 Pa s/m^2), s/c_l = 0.3

(d) Recemat (r = 8,200 Pa s/m^2), s/c_l = 0.2

(e) Recemat (r = 8,200 Pa s/m^2), s/c_l = 0.1

(f) Recemat (r = 8,200 Pa s/m^2), s/c_l = 0.05

Figure 9: Sound maps obtained for a set of airfoils at a flow speed of 81.5 m/s (M = 0.24) and a geometrical angle of attack of 4°, 4 kHz octave band

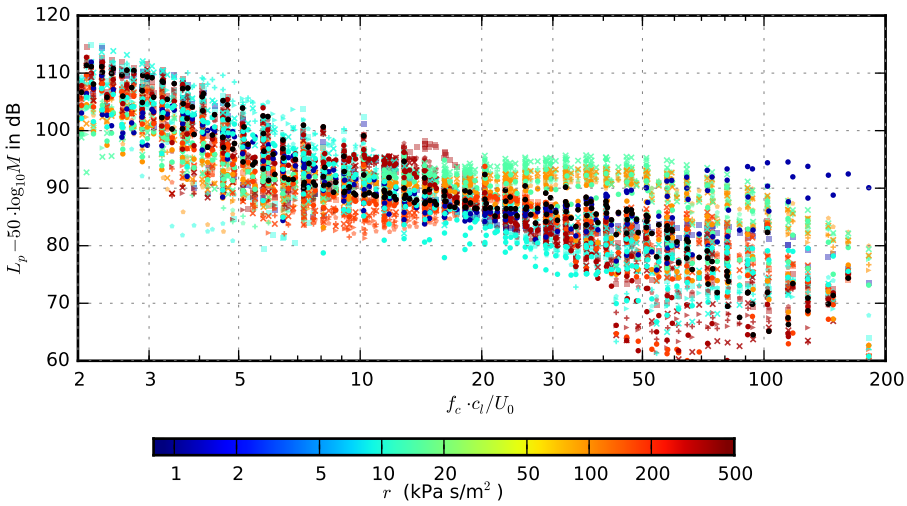

Figure 10: Scaled sound pressure level of the reference airfoil (black) and the partially porous airfoils with varying porous extent (s/c_l = ■ 0.05, ⬟ 0.1, ▸ 0.2, + 0.3, × 0.5, ● 1)

the spanwise center of the trailing edge, between two stronger noise sources that are due to the interaction of the trailing edge with the wind tunnel shear layer (see Figure 5). Basically, a reduction of the strength of this noise source due to the porous material is visible for all porous extents. Then, the sound maps also reveal that there is a noise source at the aft end of the impermeable foil, at the point where the airfoil becomes porous. With decreasing extent of the porous material (from s/c_l = 50 % in Figure 9(b) to 5 % in Figure 9(f)), this source is visible as a spanwise line moving downstream towards the trailing edge. The contribution from this noise source was also included in the following sound pressure level spectra. One idea to reduce the strength of this source in future investigations would be to use a foil with a serrated trailing edge.

A total comparison of the sound pressure levels of all airfoils of the present study is given in Figure 10. Thereby, the sound pressure level is scaled with the fifth power of the Mach number, following the theoretical work of Ffowcs Williams and Hall [21], and displayed as a function of the chord based Strouhal number. Basically, it can be seen that some airfoils lead to a noise reduction especially at low and medium Strouhal numbers, while several airfoils also lead to a noise increase at high Strouhal numbers, which is due to a contribution of surface roughness noise [4, 5]. However, it is not easy to properly analyze the results due to

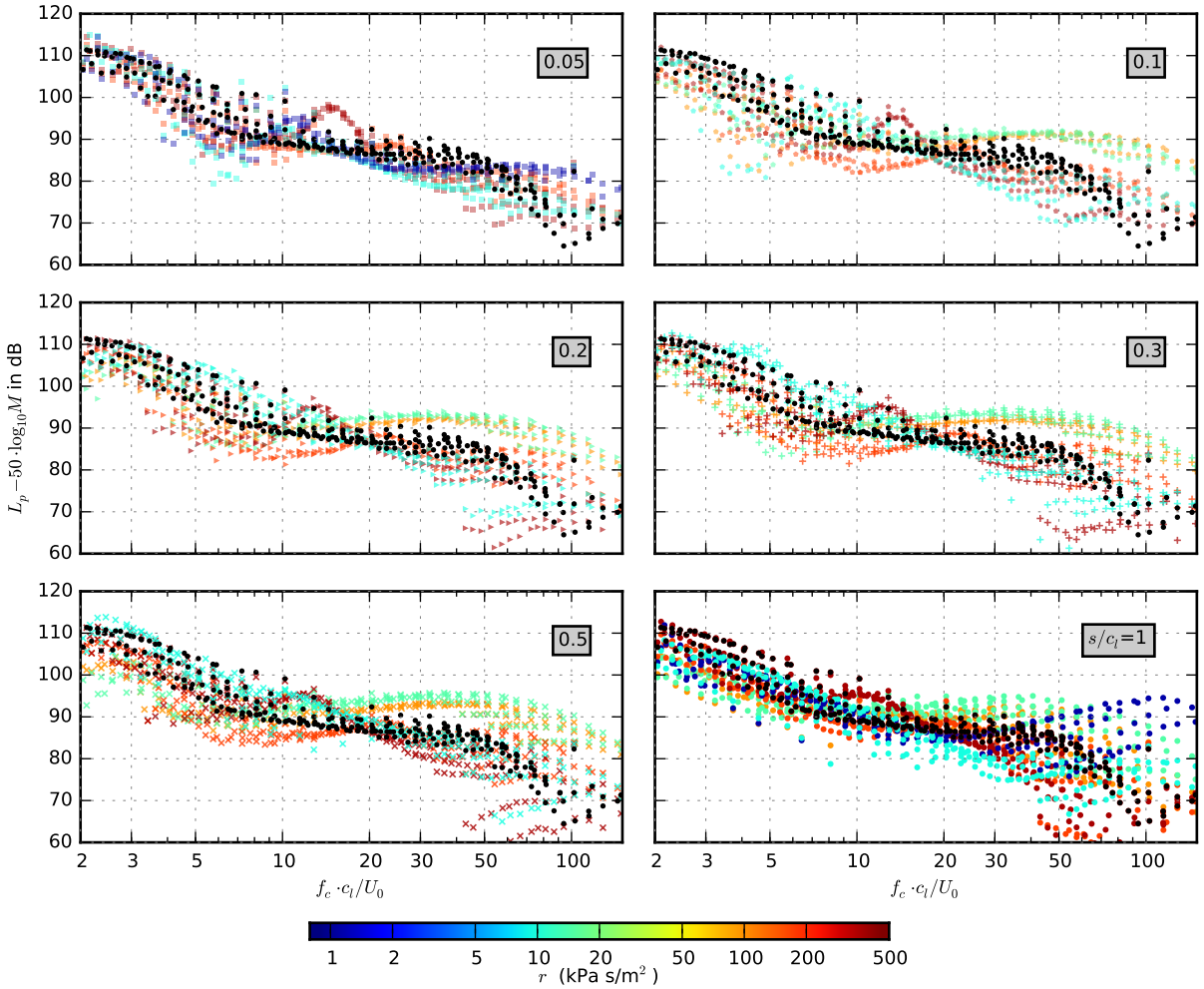

Figure 11: Scaled sound pressure level of the reference airfoil (black) and the partially porous airfoils with varying porous extent (porous materials color-coded as in Figure 7)

the large number of data. Thus, Figure 11 shows the scaled sound pressure levels sorted by the porous extent s of the airfoils and Figure 12 shows the corresponding sound pressure level difference

$$\Delta L_p = L_{p,\text{reference}} - L_{p,\text{porous}}. \tag{3}$$

The sound pressure level difference takes a positive value when the porous airfoils lead to a noise reduction compared to the reference airfoil and a negative value if they lead to a noise increase. From both Figure 11 and Figure 12, several conclusions can be drawn: Firstly, it can be seen that a high noise reduction of roughly 5 to 10 dB at low and medium Strouhal numbers can already be achieved with a very small extent of porous material (e.g. s/c_l = 0.05 or s/c_l = 0.10), which, in return, leads to only a minimum aerodynamic penalty. Secondly, as can be expected, the contribution of surface roughness noise at high Strouhal numbers increases when the extent of the porous materials increases. This, too, could be prevented when only a small (chordwise) fraction at the trailing edge of the airfoil is porous. In addition, it can be observed that some of the porous airfoils lead to a broad hump in the sound pressure level spectra in a range of Strouhal numbers between 10 and 20. This is most likely due to a contribution of bluntness noise from the aft end of the impermeable foil at $x = c_l - s$.

4. SUMMARY

The use of flow permeable materials is a known approach to reduce the aerodynamic noise generated at the trailing edge of an airfoil due to the interaction of the turbulent boundary layer with the sharp edge. The present paper describes an experimental study on airfoils with a porous trailing edge of varying (chordwise) extent. The measurements were carried out in an open jet wind tunnel using microphone array technique.

The results show that a high noise reduction of 5 to 10 dB can even be achieved with only a very small

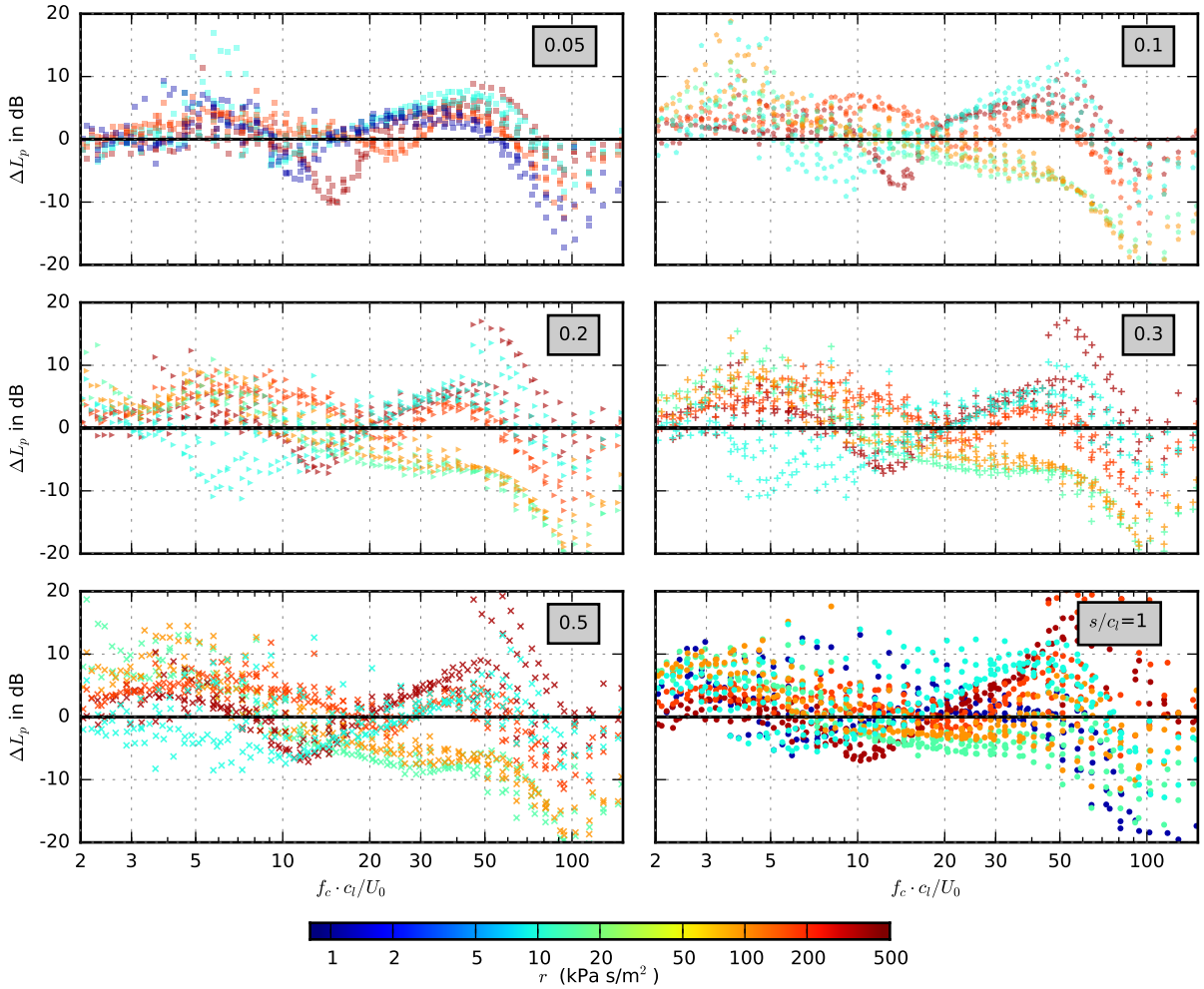

Figure 12: Sound pressure level difference of the partially porous airfoils with varying porous extent compared to the reference airfoil (porous materials color-coded as in Figure 7, positive value denotes noise reduction, negative noise increase)

extent of the porous trailing edge (for example 5 %). At the same time, a small extent of the porous edge results in a better aerodynamic performance and a smaller contribution of surface roughness noise. Thus, the selection of appropriate porous materials seems much more important regarding the design of feasible low-noise airfoils than a large chordwise extent of the porous material.

Acknowledgements

The authors thank Yangyang Ji for his help with the measurements.

REFERENCES

[1] Herr, M., Design criteria for low-noise trailing edges. In: 13th AIAA/CEAS Aeroacoustics Conference, AIAA-paper 2007-3470, 2007.

[2] Finez, A., Jondeau, E., Roger, M., Jacob, M. C., Broadband noise reduction with trailing edge brushes. In: 16th AIAA/CEAS Aeroacoustics Conference, AIAA-paper 2010-3980, 2010.

[3] Sudhakaran, R., Mimani, A., Porteous, R., Doolan, C. J., An experimental investigation of the flow-induced noise generated by a porous trailing edge of a flat plate. In: Acoustics 2015 Hunter Valley, 2015.

[4] Geyer, T. F., Sarradj, E., Fritzsche, C., Measurement of the noise generation at the trailing edge of porous airfoils. Experiments in Fluids 48, 291 - 308, 2010.

[5] Geyer T. F., Sarradj, E., Fritzsche, C., Porous airfoils: noise reduction and boundary layer effects. International Journal of Aeroacoustics, 9(6):787 - 820, 2010.

[6] Sarradj, E., Geyer, T. F., Symbolic regression modeling of noise generation at porous airfoils. Journal of Sound and Vibration, Volume 333, Issue 14, 3189-3202, 2014.

[7] Herr, M., Reichenberger, J., In search of airworthy trailing-edge noise reduction means. In: 17th AIAA/CEAS Aeroacoustics Conference, AIAA paper 2011-2780, 2011.

[8] Showkat Ali, S. A., Szőke, M., Azarpeyvand, M., Ilário da Silva, C. R., Trailing edge bluntness flow and noise control using porous treatments. In: 22nd AIAA/CEAS Aeroacoustics Conference, AIAA paper 2015-2832, 2016.

[9] Rubio Carpio, A., Merino Martinez, R., Avallone, F., Ragni, D., Snellen, M., Van der Zwaag, S., Broadband trailing edge noise reduction using permeable metal foams. In: 46th International Congress on Noise Control Engineering, INTER-NOISE, 2017.

[10] Vathylakis, A., Chong, T. P., Joseph, P. F., Poro-Serrated Trailing-Edge Devices for Airfoil Self-Noise Reduction. AIAA Journal, 53(11), 3379-3394, 2015.

[11] Kisil, A., Ayton, L. J., Aerodynamic noise from rigid trailing edges with finite porous extentions. Journal of Fluid Mechanics, 836, 117-144, 2018.

[12] Bae, Y., Moon, Y. J., Effect of passive porous surface on the trailing-edge noise. Physics of Fluids, 23, 126101, 2011.

[13] Faßmann, B. W., Rautmann, C., Ewert, R., Delfs, J. W., Prediction of porous trailing edge noise reduction via acoustic perturbation equations and volume averaging. In: 21st AIAA/CEAS Aeroacoustics Conference, AIAA paper 2015-2525.

[14] Zhou, B. Y., Gauger, N. R., Koh, S. R., Meinke, M., Schröder, W., On the adjoint-based control of trailing-edge turbulence and noise minimization via porous material. In: 21st AIAA/CEAS Aeroacoustics Conference, AIAA paper 2015-2530, 2015.

[15] Koh, S. R., Meinke, M., Schröder, W., Numerical analysis of the impact of permeability on trailing-edge noise. Journal of Sound and Vibration, 421, 348 - 376, 2018.

[16] Geyer, T. F., Sarradj, E., Trailing edge noise of partially porous airfoils. In: 20th AIAA/CEAS Aeroacoustics Conference, AIAA paper 2014-3039, 2014.

[17] ISO 9053 (1993) Acoustics – Materials for acoustical applications – Determination of airflow resistance. International Organization for Standardization

[18] Sarradj, E., Fritzsche, C., Geyer, T. F., Giesler, J., Acoustic and aerodynamic design and characterization of a small-scale aeroacoustic wind tunnel, Applied Acoustics, 70, 1073-1080, 2009.

[19] Sijtsma, P., CLEAN based on spatial source coherence. International Journal of Aeroacoustics, 6(4), 357-374, 2007.

[20] Sarradj, E., A fast ray casting method for sound refraction at shear layers. International Journal of Aeroacoustics, Vol 16, Issue 1-2, pp. 65 - 77, 2016.

[21] Ffowcs Williams, J., Hall, L. H., Aerodynamic sound generation by turbulent flow in the vicinity of a scattering half plane. Journal of Fluid Mechanics, 40(4), 657-670, 1970.